

promoting access to White Rose research papers



Universities of Leeds, Sheffield and York
<http://eprints.whiterose.ac.uk/>

This is an author produced version of a paper published in ***Optics and Lasers in Engineering*** .

White Rose Research Online URL for this paper:

<http://eprints.whiterose.ac.uk/9202/>

Published paper

Tomlinson, R.A. and Whelan, M.P. Calibration and evaluation of optical systems for full-field strain measurement. *Optics and Lasers in Engineering*, 2007, **45**(5), 550-564.

<http://dx.doi.org/10.1016/j.optlaseng.2006.08.012>

Revised manuscript for special issue of Optics and Lasers in Engineering:

CALIBRATION AND EVALUATION OF OPTICAL SYSTEMS FOR FULL-FIELD STRAIN MEASUREMENT

Eann Patterson*

Department of Mechanical Engineering, Michigan State University, USA

Erwin Hack

Laboratory of Electronics /Metrology, EMPA Duebendorf, Switzerland

Philippe Brailly

SNECMA, Safran Group, France

Richard Burguete

Airbus, UK

Qasim Saleem

Department of Mechanical Engineering, University of Sheffield, UK

Thorsten Siebert

Dantec Dynamics GmbH, Germany

Rachel Tomlinson

Department of Mechanical Engineering, University of Sheffield

Maurice Whelan

Institute for Health and Consumer Protection, European Commission DG-JRC, Italy

ABSTRACT

The design and testing of a reference material for the calibration of optical systems for strain measurement is described, together with the design and testing of a standardized test material that allows the evaluation and assessment of fitness for purpose of the most sophisticated optical system for strain measurement. A classification system for the steps in the measurement process is also proposed and allows the development of a unified approach to diagnostic testing of components or sub-systems in an optical system for strain measurement based on any optical technique. The results described arise from a European study known as SPOTS whose objectives were to begin to fill the gap caused by a lack of standards.

Keywords: optical measurement, strain, reference material, standardized test material.

* Corresponding author: 2555 Engineering Building, East Lansing, MI 48824, USA. eann@egr.msu.edu

INTRODUCTION

There have been many innovative developments in experimental mechanics in the last decade. Many of these advances involve optical techniques for the evaluation of strain and consist of either substantial improvements in the capabilities of existing techniques such as in the area of digital photoelasticity, or new techniques such as image correlation. The enthusiasm of the experimental mechanics community for these exciting innovations has not been uniformly reflected in the wider stress analysis or structural integrity communities. In these communities, a reliance on and preference for computational methods of stress and strain analysis remains the status quo. However, the need for data from experiments to validate and verify numerical models is being increasingly recognized, particularly as new materials and more complex structures provide severe challenges to reliable modeling. Despite this potential driver, there has been only a slow adoption by industry of modern optical methods for evaluating full-field strain data. One potential cause of this tardiness, and a motivation for the study described below, is the almost complete lack of standards in this field. There is an ASTM standard guide¹ which defines the terminology in the field. However, there are no internationally recognized procedures for calibrating an optical instrument used for full-field strain evaluation or for evaluating such an instrument against its design specification or comparable apparatus. The objective of the study described here was to develop devices and methodologies designed to meet both of these needs, i.e. the calibration and evaluation of optical instruments for full-field strain measurement.

The study was conducted by a consortium of eleven organizations from seven countries which was funded in part by the EU ‘GROWTH’ programme². The consortium consisted of partners from across the innovation process and included research laboratories, instrument designers, manufacturers, vendors and end-users as well national laboratories concerned with the maintenance of national and international standards. The industrial partners included both small and medium sized enterprises as well as multi-national companies from the aerospace, automotive and electronic industries. The partners were also selected to provide specialist knowledge and experience of a wide range of techniques including electronic speckle pattern interferometry (ESPI), grating

interferometry, image correlation, moiré, photoelasticity, shearography and thermoelasticity. In order to generate useful procedures with a high probability of acceptance by the technical community it was important to have good representation from the community within the study. This was achieved on at least four dimensions, i.e. trans-nationally, across the innovation process, industrial sectors, and optical techniques.

In this paper the design and supporting rationale for a reference material and a standardized test material is described. The reference material is for the calibration of optical systems of strain measurement. The standardized test material is for the evaluation of such systems and their sub-systems.

DESIGN OF REFERENCE MATERIAL

In this part of the study, the objective was to develop a device and methodology for calibrating optical systems for evaluating full-field strain data. The rational decision making model^{3,4} was used to guide the process. This model involves a number of steps that can be briefly described as: (i) identification of essential attributes, (ii) identification and weighting (in terms of importance) of desirable attributes, (iii) development of candidate designs, (iv) evaluation of candidate designs and (v) selection and embodiment of preferred design or designs. The first two stages, namely the identification of attributes was performed both within the consortium conducting the study and in consultation with the wider community. Members of the consortium were asked to identify and weight attributes for the reference material. In the wider community two groups were targeted: members of the Optical Techniques division of Society for Experimental Mechanics and attendees at the 2003 International Conference on Advances in Experimental Mechanics held in Nagoya, Japan. These two groups were asked to weight the attributes identified by the consortium. In addition, this group was given the opportunity to include additional attributes. The results obtained from this process are summarized in figure 1. There is remarkable agreement between the inputs from consortium members and the wider community which together provide representation from Asia, Europe and North America. The essential attributes were identified as those

having a weighting greater than the mean weighting plus one standard deviation (= 3.77).

Consequently the essential attributes were identified as:

- Optical access
- Exhibits no hysteresis
- In-plane capability
- Traceability to international standards
- Utilization of the length standard for traceability

Optical access and a lack of hysteresis are fairly obvious requirements when making high quality and repeatable optical measurements from which strain is being evaluated. The requirement for in-plane capability is probably an indication that most experiments to evaluate strain are performed on plane or pseudo-plane surfaces. In this case, pseudo-plane surface is taken as a curved surface that can locally be considered plane. Some techniques such as grating interferometry have been developed with this limitation as an inherent feature whilst others such as reflection photoelasticity are significantly simplified by the assumption. In this study, it was decided to restrict work to static two-dimensional strain fields because the objectives were already ambitious and most current applications would be covered despite this restriction. The concepts could be extended in the future to dynamic and three-dimensional strain fields.

Traceability is not a meaningful end in itself, but is a component of a quality assurance system. It is the ‘property of the result of a measurement or the value of a standard whereby it can be related to stated references, usually national or inter-national standards, through an unbroken chain of comparisons all having stated uncertainties’⁵. Confidence in the reliability and accuracy of an optical measuring system is in part derived from the ability to demonstrate or calibrate its performance against norms or reference materials, which are themselves founded on reliable, calibrated sources. The route through which the calibration of the reference material can be traced is relatively straightforward, or at least known, for absolute measurements such as length. Strain, defined as relative change in length, is not an absolute but a derived quantity and optical techniques measure primary quantities, e.g. birefringence or optical path length, from which strain is derived. Thus, length is the obvious measurement chain for strain though less obvious traceability

chains can be devised. However the important issue is acceptance of the traceability procedure. Traceability cannot just be claimed by a party; it must be accepted, either by virtue of the fact that an accepted standard agency sustains the calibration chain, or that the technique is accepted as traceable by virtue of its principle of operation. Accordingly based on the data in figure 1, associating strain values to the traceability chain of dimension would have a high acceptance in the community and was therefore appropriate as an essential attribute of the reference material. The requirement to make comparisons along a chain of traceability also implies that the strain distribution in the reference material should be relatively simple.

In the third stage of the rational decision making model, a number of candidate designs were developed using a series of brainstorming sessions. Initially, sixteen designs were proposed. Many of these designs were similar and so they were categorised or grouped as follows: compression geometries, diaphragms, tensile geometries and bending beams. In parallel with the first three stages of the rational decision making model, a round robin exercise was being conducted within the consortium⁶. The results of this exercise reinforced the importance of the eighth attribute from the top in figure 1: self-contained, i.e. requires no external loading. In the exercise a wide range of optical techniques were used to examine the strain field in a tensile coupon containing some complex geometric features. Many laboratories used identical models of loading machine and fixtures but enormous variability was observed in the actual loading conditions induced. Therefore, the status of this attribute was raised from desirable to essential. And, the concept of incorporating the reference material within a loading frame, as a monolithic entity, was developed. Working from the list of proposed designs, three were developed within this new concept taking account of the other essential attributes: a cantilever beam, a beam in four-point bending and a disc subject to compression across its diameter.

The reliable relative assessment of these three candidate designs against the desirable attributes was found to be too difficult and instead the beam subject to four-point bending was selected because it had been used previously in standards associated with optical measurements^{7,8}. The design of the reference material is shown in figures 2 and 3, and the extent to which it possesses the identified attributes is shown in figure 1. The

reference material can be manufactured in any material and at any scale. However, it should be noted that a calibration will only be valid for the scale of reference material utilised.

The gauge section of the reference material or specimen is the central square of dimension, $W \times W$ in the beam subject to the four-point bending. The methodology for use of the reference material recommends that this area occupies at least 90% of the area of the detector in an optical system. The beam is loaded via a set of ligaments and whiffle-trees rather than the standard knife-edges. This is necessary in order to maintain the monolithic property of the reference material, i.e. that the loading frame and specimen are a single piece of material, so that alignment is guaranteed. The integral connection creates some constraints on the beam which are not present when the loading is via knife edges. This constraint has been minimised by the design of the ligaments and use of whiffle trees which were refined using results from experiments and finite element analyses.

The reference material can be loaded in either tension or compression. In tension, load can be applied using pins in the two circular holes in the centre line. In compression, the base of the reference material is placed on a platen and load applied through the small half-cylinder on the top surface. These arrangements ensure alignment of the load which can be applied using any viable means including deadweight loading. The amount of load is monitored by measuring the relative displacement of the upper and lower halves of the outer frame of the reference material. A series of flats have been included in the top corners of the reference material to allow these measurements of displacement to be made in a variety of ways. Any calibrated displacement transducer can be employed and via its calibration provides the initial link in the traceability chain to the international standard for length. The choice of transducer will be dependent on availability and appropriateness to the scale of the reference material.

The repeatability of the measurements is important and so there should be only elastic deformation of the reference material. The interlocking system of cantilevers in the upper half of the reference material is designed to protect the specimen from plastic

deformation. The dimension of the slit, χ will be a limiting factor in manufacturing the reference material at small scales and could be enlarged but this would remove the overload protection.

DESIGN OF STANDARDISED TEST MATERIALS

The need addressed by standardised test materials is the capability to evaluate the performance and fitness for purpose of optical systems for strain evaluation. This capability would be of value to system designers in evaluating prototypes, instrument manufacturers for quality control, instrument purchasers in comparing the performance of competitive systems and end-users in setting up and adjusting apparatus. Assistance in diagnostic activities would be beneficial to nearly all of these groups and so the ability to assess the performance of sub-systems was also deemed to be appropriate. These sub-systems could be devices, such as a camera, or an algorithm such as an unwrapping procedure. The ability to make comparative evaluations of systems employing different optical techniques was an objective. This inferred the need for a unified approach to standardised tests that would be applicable to all optical techniques. In order to understand the implications of the need for a unified approach, the steps involved in the acquisition of images and processing to generate maps of strain were considered for a wide range of optical techniques for strain measurement. It was found that it was possible to classify these steps using a single classification system which is shown schematically in the central portion of figure 4. The steps which usually correspond to components or sub-systems of the optical system steps are shown as black boxes. The data produced as output from each step is shown in an oval. Generic terminology has been used for both steps and outputs. Examples of the outputs from each step are shown for a typical analysis using ESPI in a cracked compact tension specimen⁹ in the left side of figure 4. As might be expected in a classification system, not every technique will make use of every step. The way that a set of six optical techniques map onto the classification system is illustrated schematically in figure 5.

In order to evaluate each step of the measurement process it is necessary to have standard data sets to use as inputs to each step and for comparison with the outputs. Thus, a complete collection of data sets corresponding to the outputs from each step is required. This concept is illustrated on the right side of figure 4. For convenience, each data set in the collection should be connected via a theoretical relationship. These relationships will be different for each optical technique but it is possible to construct a pathway of functions leading from an initial strain distribution to the data sets shown in figure 4. By way of example, such a pathway is shown in figure 6 for digital photoelasticity using phase-stepping in circularly polarised light¹⁰. The pathway starts from an analytical model that corresponds to the standardised test material.

The design of the standardised test material followed a similar route to the one described above for the reference material, except that the wider community was not involved in identifying another set of attributes. The assessment of the performance or fitness for purpose of a strain analysis system implies the need for complex strain patterns that will present challenges for the most sophisticated instrument. The following types of strain distribution were identified as presenting the greatest challenges based on the experience of the instrument designers and end-users within the consortium conducting the study:

- Rotation of strain direction
- Strain concentration
- Free boundaries
- Discontinuity in strain
- Sign reversal in strain

Brain-storming sessions were used to generate ten candidate designs which were reviewed against the above requirements and the attributes required of the reference material, excluding traceability. A disc in diametral compression against an elastic half-space was chosen as the physical standardised test material. This geometry was incorporated into a loading frame to form a monolithic specimen as shown in figure 7. The test material can be manufactured at any scale. The gauge area is the two quadrants of the disc in contact with the half-space and the corresponding area in the half-space as shown in figure 8. The disc is mounted on a beam in order to generate a larger and more

easily measured relative displacement of the upper and lower halves of the frame and to create some rigid body displacement which is an attribute in figure 1. This rigid body displacement can be almost eliminated by using the test material upside down as in figure 13. Since contact of two initially separate components is involved, the monolithic property of the test material is achieved via two pairs of leaf springs. These springs offer almost no resistance to vertical motion but maintain the alignment within the test material. The test material can be loaded only in compression by placing it on a platen and preferably placing a dowel in the semi-circular groove on the top face. Any form of loading including dead-weights may be used. The applied load is measured by monitoring the relative displacement of the upper and lower halves of the frame at the flats provided in the top corners. This approach is identical to that used for the reference material, except in this case the rate of change of displacement must be monitored in order to detect the load at contact of the disc and half-space. The contact causes a significant change in the stiffness of the test material. A set of interlocking cantilevers protect the test material from excessive plastic deformation. At very small scales the slit, χ dimension and the leaf springs may not be scaled due to the difficulties associated with manufacturing them.

STRAIN FIELDS FOR COMPARISON

The central portion of the beam subject to four-point bending is the gauge section in the reference material shown in figures 2 and 3. The strain distribution in this gauge section can be modelled using the theory of elasticity. The simple theory of bending can be employed to describe the Cartesian strain components as:

$$\varepsilon_{xx} = \frac{yd}{6W^2} \quad \varepsilon_{yy} = \frac{-\nu yd}{6W^2} \quad \varepsilon_{xy} = 0 \quad (1)$$

where W is the depth of the beam, y is the distance from the neutral axis of the beam towards the top, d is the applied displacement load (positive for compression), and ν is Poisson's ratio. The constraint of the ligaments at the loading points could introduce

additional moments into the beam. These moments would be proportional to the applied load, such that the moment in the gauge was $\kappa P(3W)$, where P is the force applied at load point, $3W$ is the distance between the inner and outer loading points on each side of the beam and κ is a factor to account for the additional moment due to the constraint. $\kappa = 1$ when there is no constraint, and results from experiments and finite element analyses suggest that $\kappa = 0.95$ for the design shown in figure 2. There may also be some lateral tension introduced into the beam but experiments suggested that this effect was negligible. Thus, with constraint present the above expressions can be modified as follows:

$$\varepsilon_{xx} = \frac{yd\kappa}{6W^2} \quad \varepsilon_{yy} = \frac{-\nu yd\kappa}{6W^2} \quad \varepsilon_{xy} = 0 \quad (2)$$

The reporting of results can be simplified using the derivative of strain with respect to y , the distance from the neutral axis and the derivative of this quantity with respect to displacement load, i.e.

$$\frac{\partial \varepsilon_{xx}}{\partial y} = \frac{d\kappa}{6W^2} \quad \frac{\partial \varepsilon_{yy}}{\partial y} = -\frac{\nu d\kappa}{6W^2} \quad (3)$$

and

$$\frac{\partial}{\partial d} \left(\frac{\partial \varepsilon_{xx}}{\partial y} \right) = \frac{\kappa}{6W^2} \quad \frac{\partial}{\partial d} \left(\frac{\partial \varepsilon_{yy}}{\partial y} \right) = -\frac{\nu \kappa}{6W^2} \quad (4)$$

The quantities in equations (2-4) are a property of the reference material which should be constant with respect to x in the gauge section.

For the standardised test material, analytical expressions exist for the two areas shown in figure 8. The stress field in the central portion of the disc, i.e. at a distance from the points of application of load has been described by Frocht¹¹ and these expressions can be readily transformed to describe the strain field:

$$\begin{aligned}
\varepsilon_{xx}(x, y) &= -\frac{2P}{E\pi B} \left[\frac{x^2(R-y) - \nu(R-y)^3}{r_1^4} + \frac{x^2(R+y) - \nu(R+y)^3}{r_2^4} - \frac{(1-\nu)}{2R} \right] \\
\varepsilon_{yy}(x, y) &= -\frac{2P}{E\pi B} \left[\frac{(R-y)^3 - \nu x^2(R-y)}{r_1^4} + \frac{(R+y)^3 - \nu x^2(R+y)}{r_2^4} - \frac{(1-\nu)}{2R} \right] \quad (5) \\
\varepsilon_{xy}(x, y) &= \frac{2P(1+\nu)}{E\pi B} \left[\frac{(R-y)^2 x}{r_1^4} - \frac{(R+y)^2 x}{r_2^4} \right]
\end{aligned}$$

where the origin is taken at the centre of the disc and P is the load applied to the disc, E is the Young's modulus, $R=D/2$ is the radius of the disc, B is the thickness of the disc, ν is Poisson's ratio, and

$$r_1^2 = x^2 + (R-y)^2 \quad (6)$$

$$r_2^2 = x^2 + (R+y)^2$$

The subsurface stresses for a cylinder on an elastic half-space can be solved analytically¹² and again transformed to strains. In the case of normal and tangential loading, the subsurface strain field is given for a static or sliding line contact for identical materials by:

$$\begin{aligned}
\varepsilon_{xx} &= \left[\frac{Py_n^2}{\pi ED(1-\nu^2)} \right]^{1/2} \left[2 - \frac{\zeta}{(1+\zeta^2)^{1/2}} - \frac{(1+\zeta^2)^{1/2}}{\zeta} - \frac{x_n^2 \zeta^3}{(1+\zeta^2)^{3/2}(\zeta^4 + y_n^2)} \right] \\
&+ \left[\frac{P\mu^2}{\pi ED(1-\nu^2)} \right]^{1/2} \left\{ \frac{(1+\nu)x_n y_n^2 \zeta}{(1+\zeta^2)^{1/2}(\zeta^4 + y_n^2)} - 2x_n \left[1 - \frac{\zeta}{(1+\zeta^2)^{1/2}} \right] \right\} + \left[\frac{Py_n^6}{\pi ED(1-\nu^2)} \right]^{1/2} \left[\frac{\nu(1+\zeta^2)^{1/2}}{\zeta(\zeta^4 + y_n^2)} \right]
\end{aligned}$$

$$\begin{aligned}
\varepsilon_{yy} = & \left[\frac{P\mu^2}{\pi ED(1-\nu^2)} \right]^{1/2} \left[\frac{x_n y_n^2 \zeta}{(1+\zeta^2)^{1/2} (\zeta^4 + y_n^2)} \right] + \left[\frac{P y_n^6}{\pi ED(1-\nu^2)} \right]^{1/2} \left[\frac{(1+\zeta^2)^{1/2}}{\zeta (\zeta^4 + y_n^2)} \right] \\
& - \left[\frac{\nu^2 P y_n^2}{\pi ED(1-\nu^2)} \right]^{1/2} \left[2 - \frac{\zeta}{(1+\zeta^2)^{1/2}} - \frac{(1+\zeta^2)^{1/2}}{\zeta} - \frac{x_n^2 \zeta^3}{(1+\zeta^2)^{3/2} (\zeta^4 + y_n^2)} \right] \\
& - \left[\frac{\nu^2 P \mu^2}{\pi ED(1-\nu^2)} \right]^{1/2} \left\{ \frac{x_n y_n^2 \zeta}{(1+\zeta^2)^{1/2} (\zeta^4 + y_n^2)} - 2x_n \left[1 - \frac{\zeta}{(1+\zeta^2)^{1/2}} \right] \right\}
\end{aligned} \tag{7}$$

$$\varepsilon_{xy} = \left(\frac{P(1+\nu)^2}{\pi ED(1-\nu^2)} \right)^{1/2} \left[\frac{-x_n y_n^2 \zeta}{(1+\zeta^2)^{1/2} (\zeta^4 + y_n^2)} + \mu \left\{ y_n \left[2 - \frac{\zeta}{(1+\zeta^2)^{1/2}} - \frac{(1+\zeta^2)^{1/2}}{\zeta} - \frac{x_n^2 \zeta^3}{(1+\zeta^2)^{3/2} (\zeta^4 + y_n^2)} \right] \right\} \right]$$

where

$$\zeta^2 = \frac{1}{2} \left\{ -\left(1 - x_n^2 - y_n^2\right) + \left[\left(1 - x_n^2 - y_n^2\right)^2 + 4y_n^2 \right]^{1/2} \right\} \tag{8}$$

and the co-ordinate system (x,y) is defined from the centre of contact with the y -axis being positive into the elastic half-space, (x_n, y_n) are values normalised by the contact half-length b_c and μ is the coefficient of friction.

METHODOLOGIES FOR USE

The reference material and standardized test material should be manufactured to the tolerances specified in figures 2 and 7 and following manufacture they should be measured to establish the actual dimensions of the gauge section and surrounding areas. The uncertainty of these measurements, $u^2(f)$ should be estimated in millimetres.

The requirements for calibration using the reference material are much more rigorous than for evaluation using the standardized test material. For the standardized test material the level of comparison will depend on the purpose for using the test material. Consequently the user can make a decision on the extent to which the procedure for the reference material is followed using the corresponding analytical expressions. An

important difference is that the analytical models described by Lamé's equations and (5) to (9) are used as the starting point in the pathways of functions leading to the standardized data sets as shown by the example in figure 6.

For the reference material, the thickness, B , depth, W and distance between the loading points, a and c (see figure 9) should all be measured and the uncertainty estimated¹³. It is recommended that the measured strain distribution should be compared with the predicted values obtained from expression (2) by plotting the difference between measured and predicted values as a function of x and y in the gauge area. A linear least-squares fit to the field of deviations, $\Delta(i, j)$ yields an offset A_0 and calibration factor A_1 for each load step by minimizing the residual below:

$$\sum_{i,j} [\Delta(i, j) - A_0 - A_1 y_j]^2 \quad (10)$$

The fit-parameters to be reported are calculated from

$$A_0 = \frac{1}{N} \sum_{i,j} \Delta(i, j) \quad A_1 = \frac{\sum_{i,j} y_j \Delta(i, j)}{\sum_{i,j} y_j^2} \quad (11)$$

Also the mean square residual deviation can be calculated after the linear fit by using

$$u^2(\Delta(k)) = \frac{1}{N} \sum_{i,j} [\Delta(i, j)]^2 - A_0^2 - A_1^2 \frac{1}{N} \sum_{i,j} y_j^2 \quad (12)$$

and the uncertainties of the fit-parameters should be reported as

$$u^2(A_0) = \frac{1}{N} u^2(\Delta) \quad u^2(A_1) = \frac{u^2(\Delta)}{\sum_{i,j} y_j^2} \quad (13)$$

Ideally both A_0 and A_1 are zero.

The uncertainty in the reference material can be calculated using:

$$\begin{aligned}
u_{RM}^2(\varepsilon_{xx}) &= \left(\frac{d}{6W^2}\right)^2 y^2 \left[\frac{u^2(d)}{d^2} + \frac{16u^2(W) + u^2(a) + u^2(c)}{4W^2} \right] \\
u_{RM}^2(\varepsilon_{yy}) &= \left(\frac{\nu d}{6W^2}\right)^2 y^2 \left[\frac{u^2(d)}{d^2} + \frac{16u^2(W) + u^2(a) + u^2(c)}{4W^2} + \frac{u^2(\nu)}{\nu^2} \right]
\end{aligned} \tag{14}$$

Similar expressions associated with the sum and difference of the principal strains as well as other components of strain can be deduced. Complete derivations of these expressions and others given here are available elsewhere¹⁴. Finally the calibration uncertainty is given by:

$$u_{cal}^2(\varepsilon_{xx}) = u_{RM}^2(\varepsilon_{xx}) + u^2(\Delta) \tag{15}$$

The measurement uncertainty in a future experiment performed with the unchanged measurement system is at least as high as the calibration uncertainty found using the procedure above.

DISCUSSION

The design of these materials did not follow a straight path but as in all design processes involved the testing of prototypes and the refinement of the designs. In this case prototypes were tested using multiple optical techniques in several countries. Finite element analysis was also performed to aid the understanding of the behavior observed. The sample results from the reference material are shown in figures 10 to 12. These results were obtained in different laboratories by different investigators without the use of a detailed protocol for the experiments. The specimens employed were manufactured by two partners in the consortium conducting the study. In one set, the dimensions were $B=W=20\text{mm}$ where B is the depth out-of plane in figure 2 and in the other $W=29\text{mm}$. In the light of these circumstances, there is remarkable agreement between the results.

Figure 10 shows one of the specimens set-up for analysis using ESPI. The left graph in figure 11 shows a comparison of results from a strain gauge rosette bonded to the underside of the gauge-section with results from finite element analyses carried out

independently by separate laboratories with the analytical solution. The right graph in Figure 11 shows results from ESPI, image correlation and strain gauges plotted together with the finite element results and analytical solution in the form of the derivative of expression (1) as a function of the applied displacement. It is clear from these results that both close proximity to theory and reproducibility have been achieved. However, data from photoelasticity and thermoelasticity plotted in terms of stresses in figure 12 suggest that there are some differences relative to the analytical result although there is close agreement with the finite element results. These findings imply the boundary conditions on the test beam do not correspond perfectly to those assumed by the simple bending theory and as a consequence the whiffle-trees were re-designed to reduce their stiffness as shown in figure 2.

Similar tests were conducted on the standardized test material. Specimens made of three materials (stainless steel, aluminium, and SLA polymer) with three different sizes of the disk (diameter of $D=10, 50$ and 100mm) were analysed. Only photoelasticity applied to the largest specimen generated good quality results (figure 14) in all the areas of analysis shown in figure 8. The other techniques utilised were not able to resolve reliably the strain data in all of the areas. The data in figure 14 was obtained from a specimen with $D=100\text{mm}$ made from epoxy resin using stereolithography. A photoelastic coating of thickness 0.001 m was applied in the gauge regions and the phase-stepping technique⁹ used to generate quantitative maps of principal strain difference at three increments of applied load, $P = 795, 1590,$ and 2395N .

The standardized test was designed to allow the capabilities of the most sophisticated optical systems to be evaluated. The inability of most techniques to resolve all of the strain features simultaneously demonstrates that the objective has been achieved. It was possible for most techniques to process part of the strain distribution at all scales.

CONCLUSIONS

The design of a reference material for the calibration of optical systems for strain measurement has been proposed together with the design of a standardized test material. Experiments performed using the materials and employing a wide range of optical techniques at a number of scales suggest they are achieving their objectives. These materials have arisen from a European study which has proposed a draft standard¹⁴ incorporating details of these designs and methodologies for their use. Adoption and use of these materials should lead to an improvement in the quality of data generated by optical systems for strain measurement and to significantly enhanced confidence in the data. These outcomes will be of benefit to both the experimental mechanics community and to the wider technical community.

ACKNOWLEDGEMENTS

The authors gratefully acknowledge the substantial contributions of the partners in the SPOTS project: Airbus, CRF Societa Consortile per Azioni, Dantec Dynamics, EC-JRC-IHCP, Eidgenössische Materialprüfungs-und Forschungsanstalt (EMPA), Honlet Optical Systems GmbH, NPL Management Limited, Optical Metrology Innovations, Politechnika Warszawska, SNECMA, and the University of Sheffield. The project was supported by EU grant: G6RD-CT-2002-00856 ‘SPOTS’ and the Swiss Federal Office for Education and Science.

REFERENCES

- 1 ASTM E2208-02 (2002) *Standard Guide for evaluating non-contacting optical strain measurement systems*, ASTM International, West Conshohocken, PA, USA.
- 2 SPOTS "Standardisation project for optical techniques of strain measurement", EU contract no. G6RD-CT-2002-00856, (see <http://www.opticalstrain.org>)
- 3 Cross, N., *Engineering Design Methods*, John Wiley & Sons, London, 1989.
- 4 Olden, E.J., Patterson, E.A., 'A rational decision making model for experimental mechanics', *Experimental Techniques*, 24(4): 26-32, 2000.
- 5 International vocabulary of basic and general terms in metrology (VIM) (1994), ISO/IEC/OIML/BIPM
- 6 Mendels, D. –A., Hack, E., Siegmann, P., Patterson, E.A, Salbut, L., Kujawinska, M., Schubach, H.R., Dugand, M., Kehoe, L., Stochmil, C., Brailly, P., Whelan. M., 2004, 'Round robin exercise for optical strain measurement', *Proc. 12th Int. Conf. Exptl. Mechanics, Advances in Experimental Mechanics*, edited by C. Pappalettere, McGraw-Hill, Milano, pp.695-6.
- 7 ASTM C1377-97, *Standard test method for calibration of surface stress measuring devices*, ASTM International, West Conshohocken, PA, USA.
- 8 ASTM C770-98, *Standard test method for measurement of glass stress-optical coefficient*, ASTM International, West Conshohocken, PA, USA.
- 9 Shterenlikht, F.A. Diaz Garrido, P. Lopez-Crespo, P.J. Withers, E.A. Patterson, "SIFs from strain fields using ESPI and image correlation", *Proc. SEM Int. Congress Exptl. Mech.*, Costa Mesa, California, 2004.
- 10 Patterson, E. A., 2002, 'Digital photoelasticity: principles, practice and potential', *Strain*, 38: 27-39.
- 11 Frocht, M.M., *Photoelasticity, vol.II*, John Wiley & Sons, New York, 1948, p.121-6.
- 12 Hills, D. A., Nowell, D. Sackfield, A., *Mechanics of Elastic Contacts*. Butterworth Heinemann, Oxford, 1993.
- 13 ISO 17025, *Guide to the expression of uncertainty in measurements*, ISO Geneva, Switzerland, October 1993.
- 14 SPOTS Standard Part 1 & 2, *Calibration and assessments of optical strain measurements*, www.opticalstrain.org 2006.

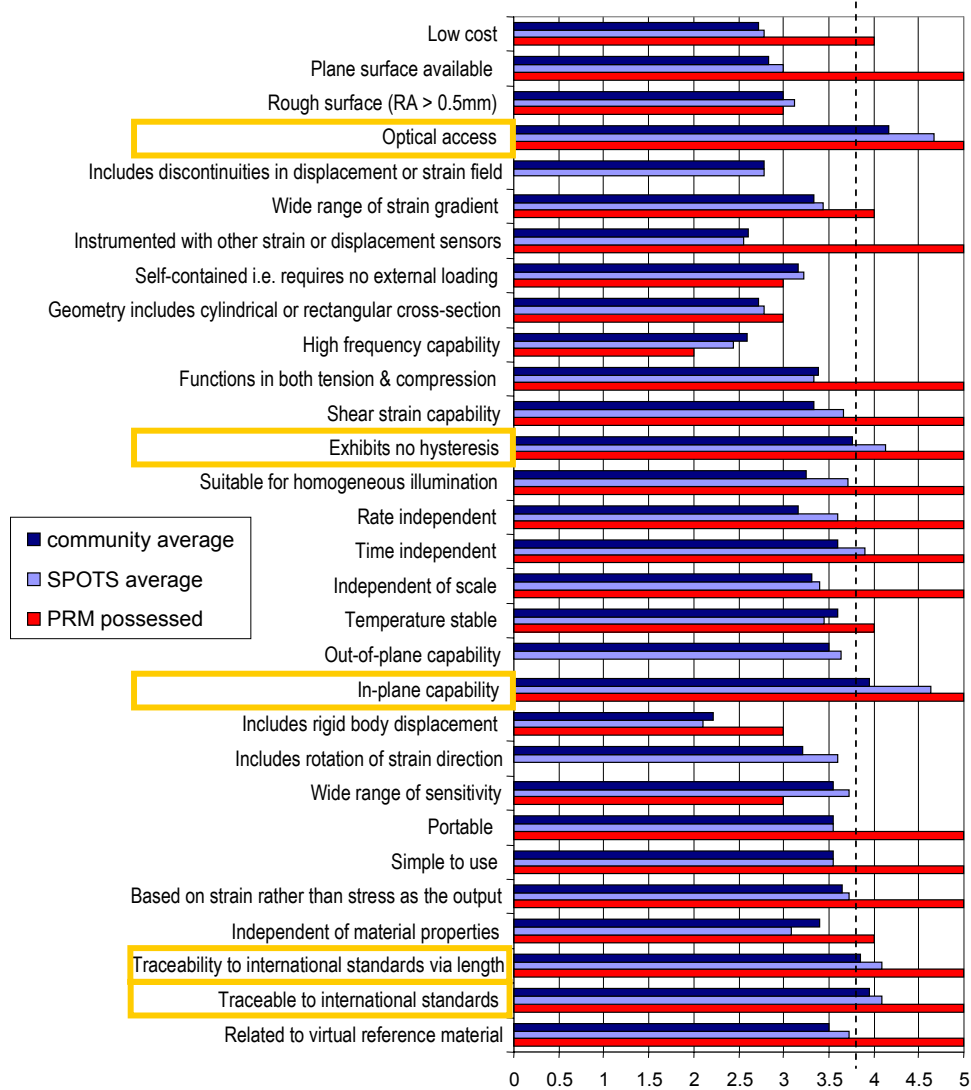


Figure 1 – Attributes and their weightings for the reference materials together with the extent to which they are possessed by the selected design. The weightings (1 - unimportant, 2 - preferred, 3 - important, 4 - highly desirable, or 5 – essential) assigned by individual partners in the study were averaged and the same exercise repeated for the wider community including the partners. Essential attributes were identified as those having an average weighting from the whole community greater than the mean plus a standard deviation of the weightings (broken line) and are highlighted above. The extent to which an attribute was possessed by the new reference material were assessed as 5 – completely possessed, 4 – to a large degree, 3 – to some degree, 2 – to a limited degree or in some circumstances, 1 – not possessed but could be arranged, 0 – not possessed at all.

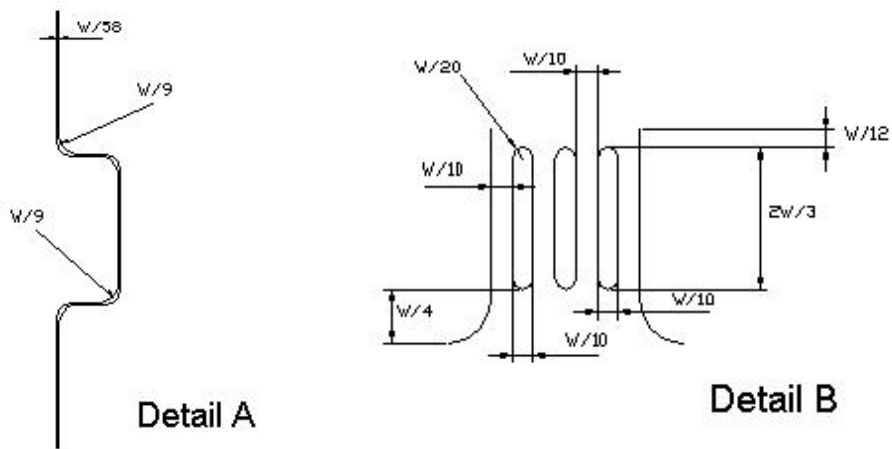
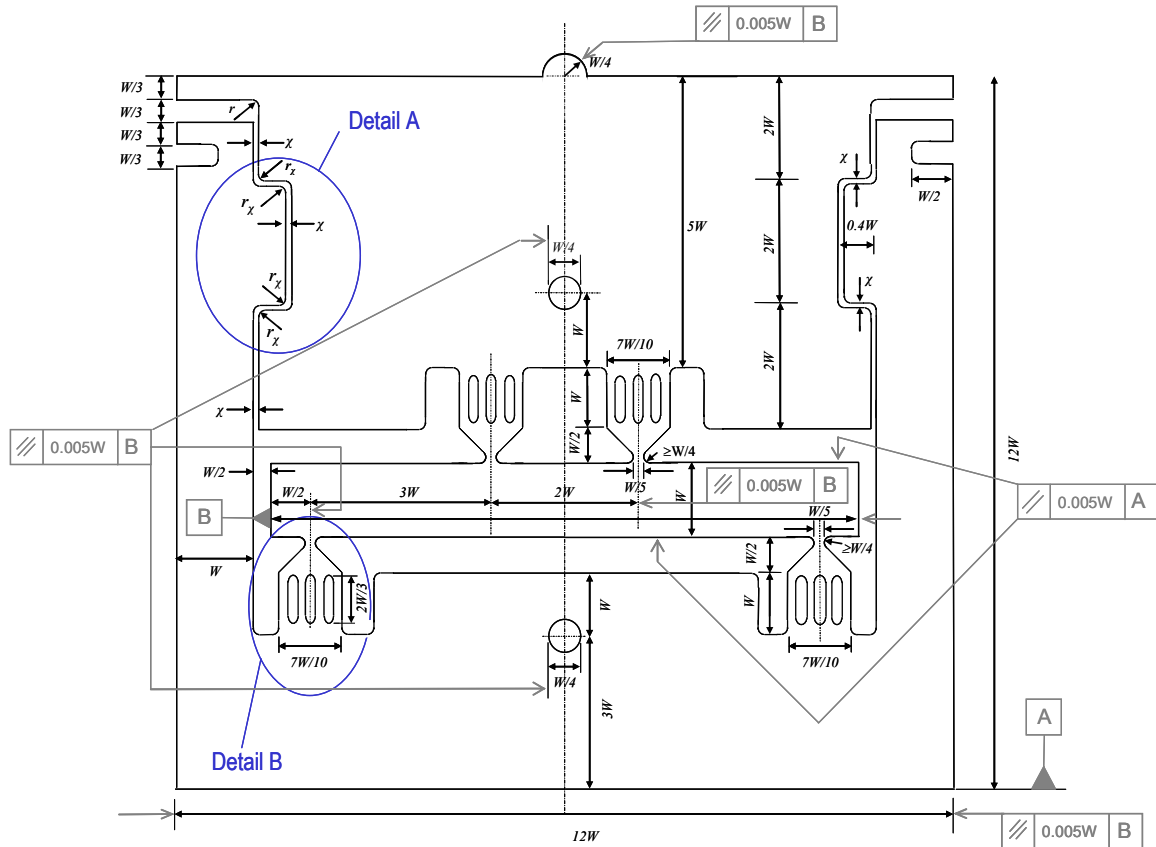


Figure 2 – Schematic of the reference material with normalised dimensions. All radii are $(W/5)$ unless otherwise specified and the thickness B is $0.2W \leq B \leq W$. Tolerances should be 0.05mm unless otherwise specified including the parallelism of the front and back faces. (EU Community Design Registration 000213467).

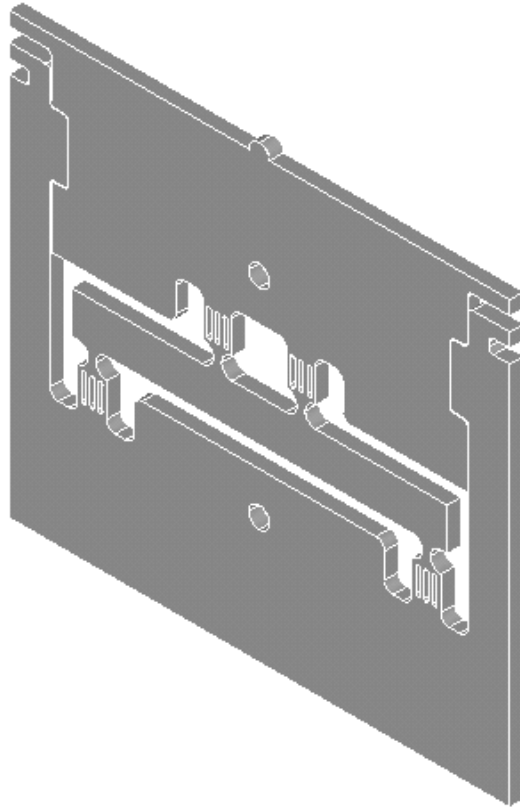


Figure 3 – Three dimensional view of reference material (*EU Community Design Registration 000213467*).

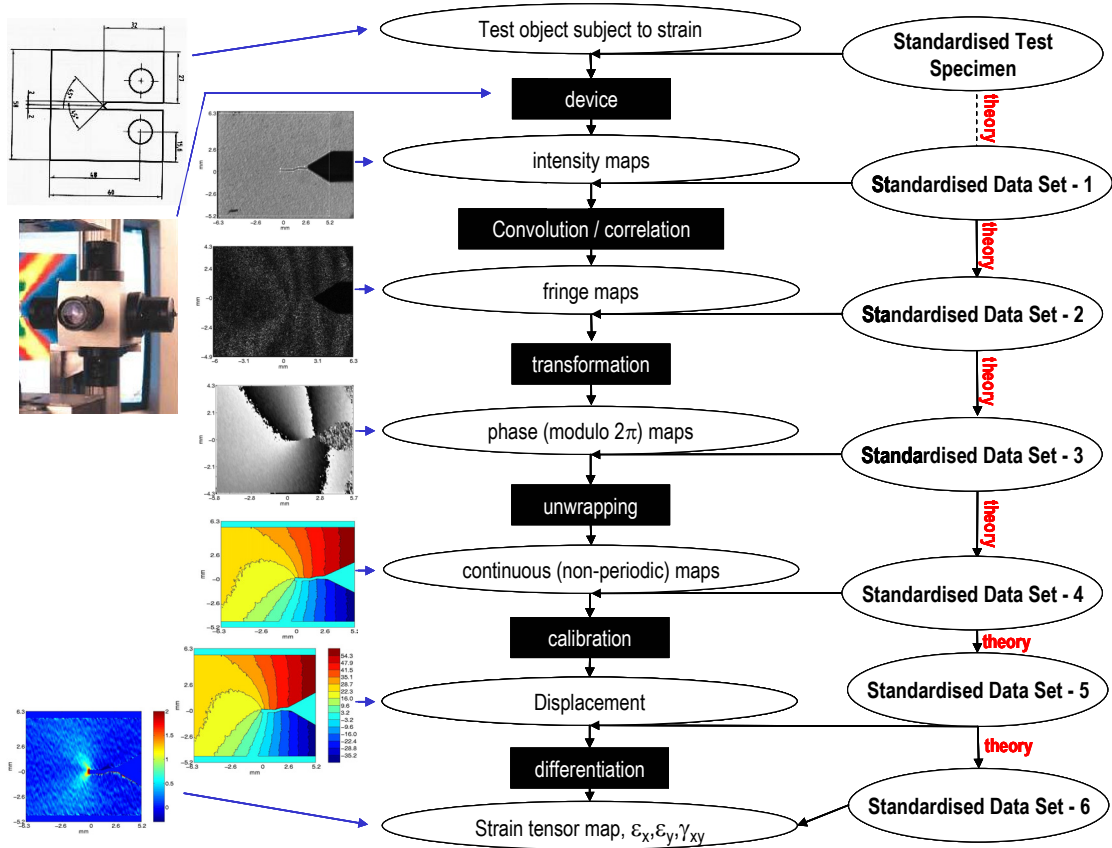


Figure 4 – A schematic illustrating the classification system for steps in the measurement process (*centre*) for optical strain measurement systems and the relationship to the proposed standardized test and data sets (*right*). The ovals represent data sets and the rectangles represent components of the system. The process is exemplified (*left*) using measurements of the y-direction (vertical) strain in a cracked compact tension specimen from ESPI.

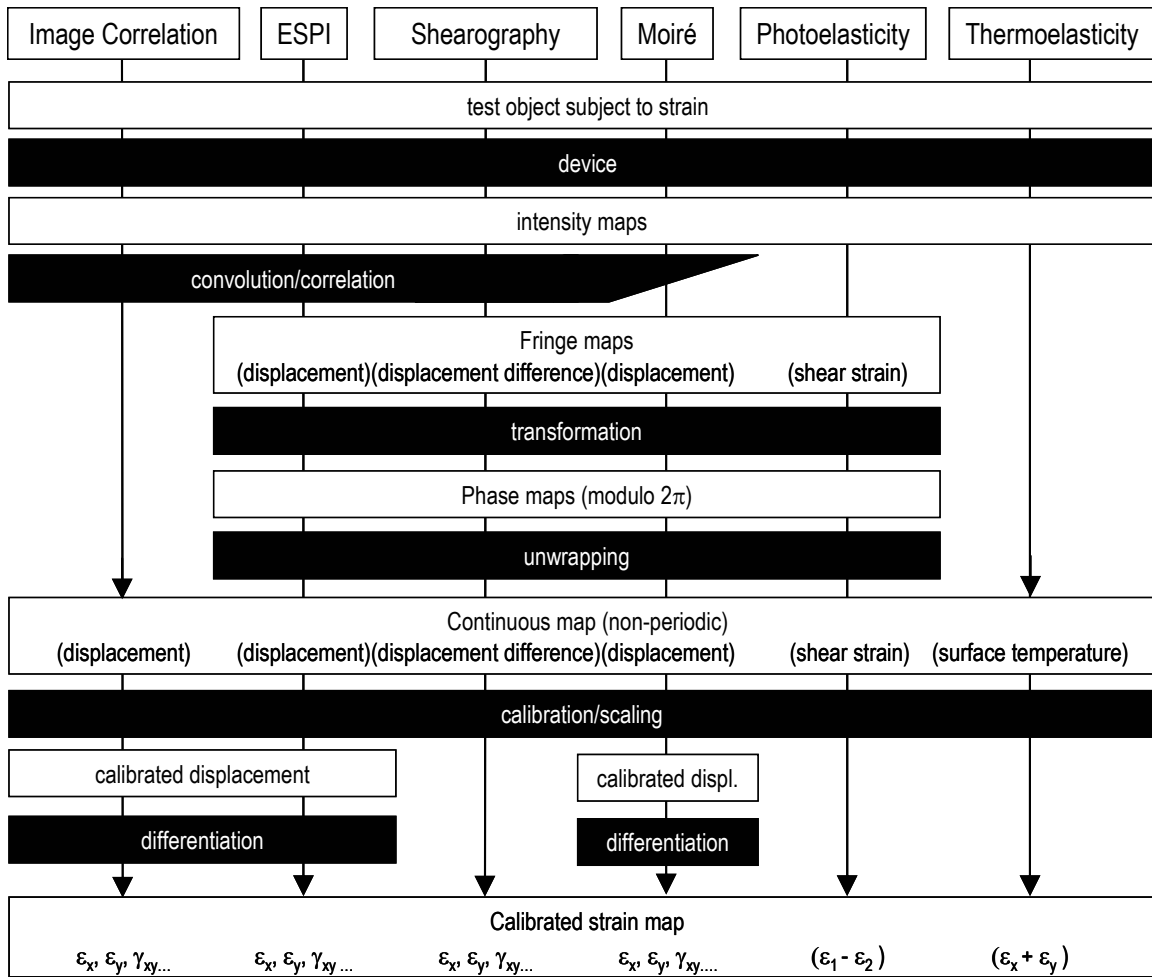


Figure 5 – Schematic illustration showing how a range of optical techniques for strain measurement map onto the classification system shown in figure 4. The steps in the measurement process are shown as black boxes and the output data from a step as white boxes.

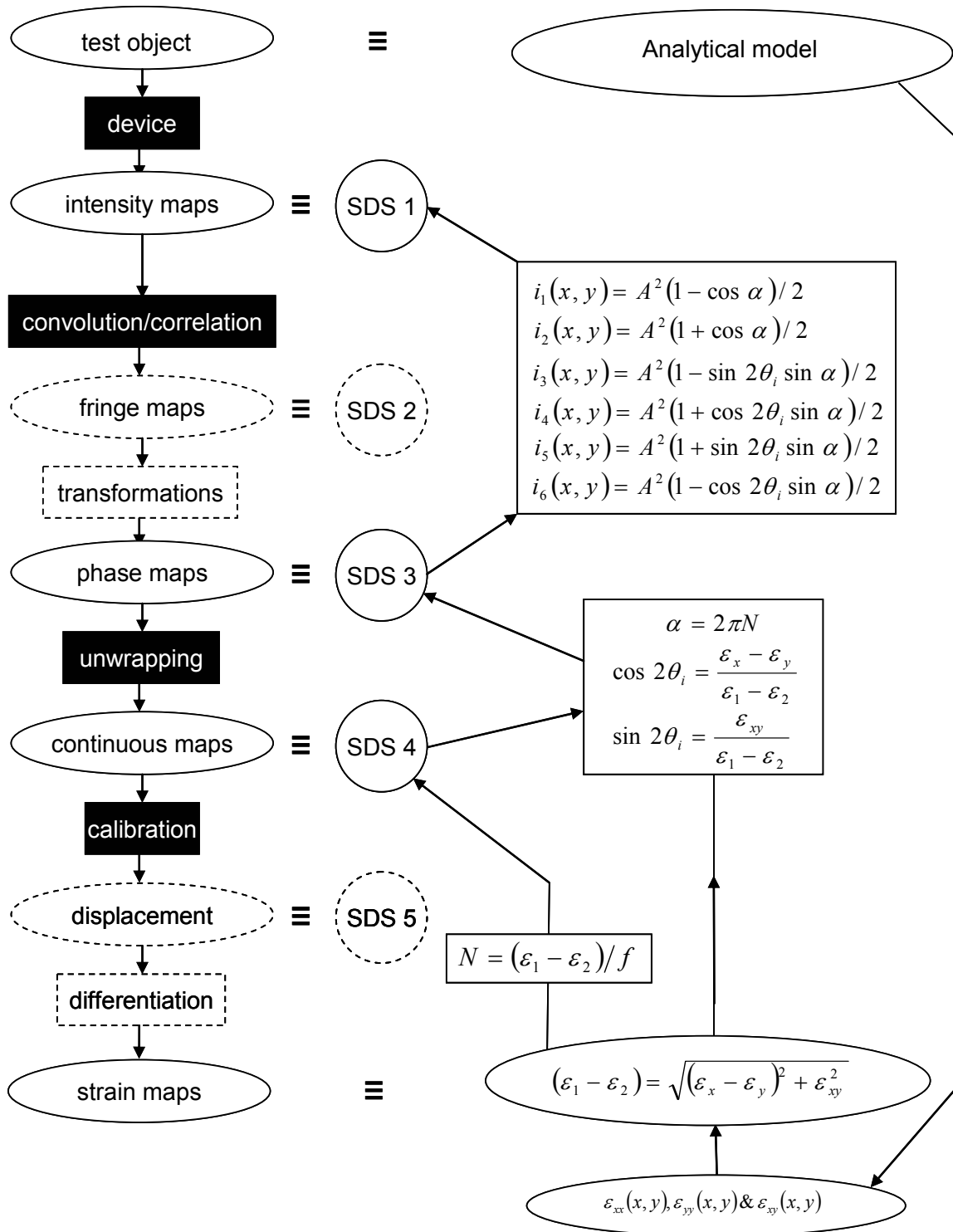


Figure 6 – Schematic showing the classification system (left) from figure 4 customized for digital photoelasticity with the pathway of functions (right) required to generate the standardized data sets (SDS) using an known strain distribution from an analytical model.

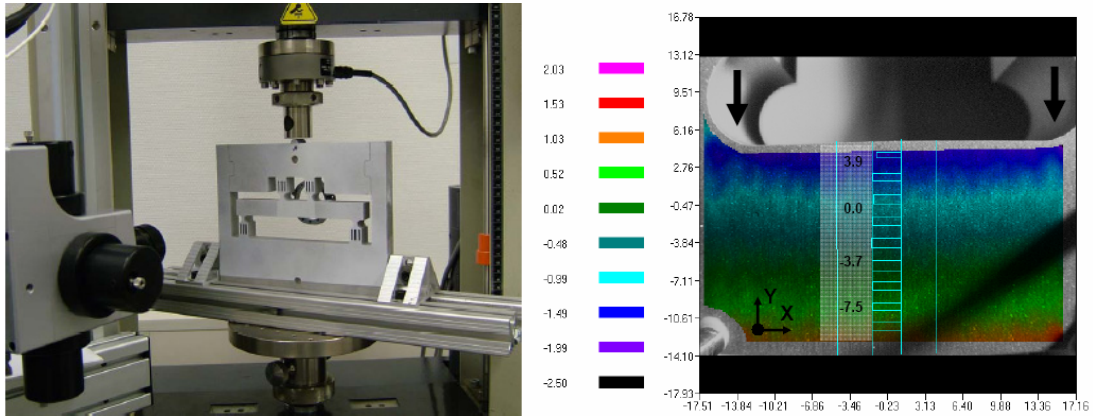


Figure 10 – Prototype reference material set-up for analysis using ESPI system (*left*) and results (*right*) for ϵ_{xx} in the gauge-section.

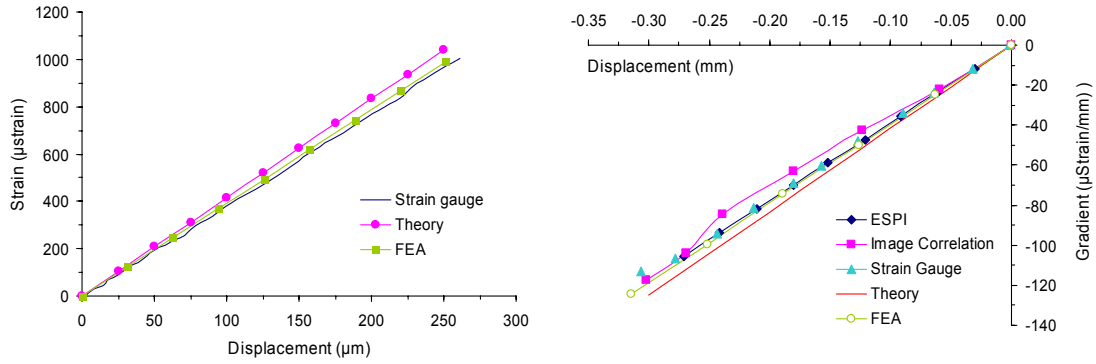


Figure 11 – Experimental results from the reference material showing a comparison (*left*) of strain gauge and finite element results with theory of elasticity for the underside of the gauge-section and the relationship (*right*) between the strain gradient across the width of the gauge-section as a function of applied displacement obtained using ESPI, image correlation, strain gauges and finite element analysis.

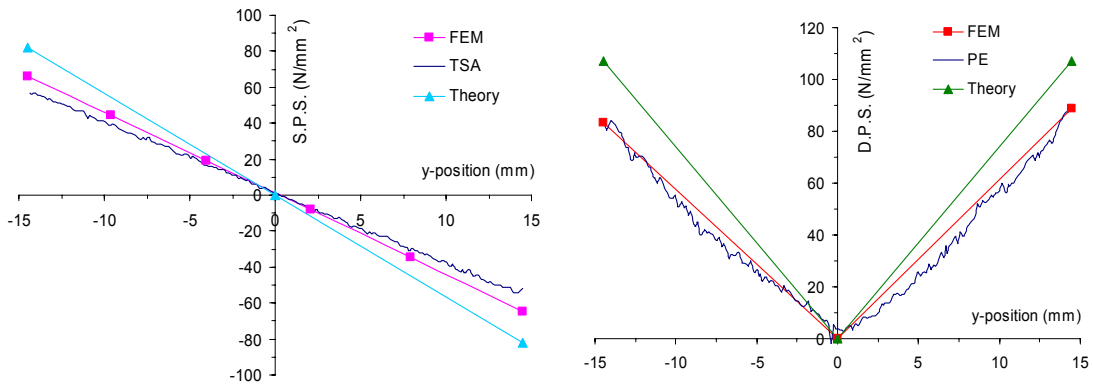


Figure 12 – Experimental results for the reference material from thermoelastic stress analysis (*left*) and photoelasticity (*right*) for the sum (SPS) and differences (DPS) respectively of the principal stresses with results from finite element analysis and theory of elasticity for comparison.

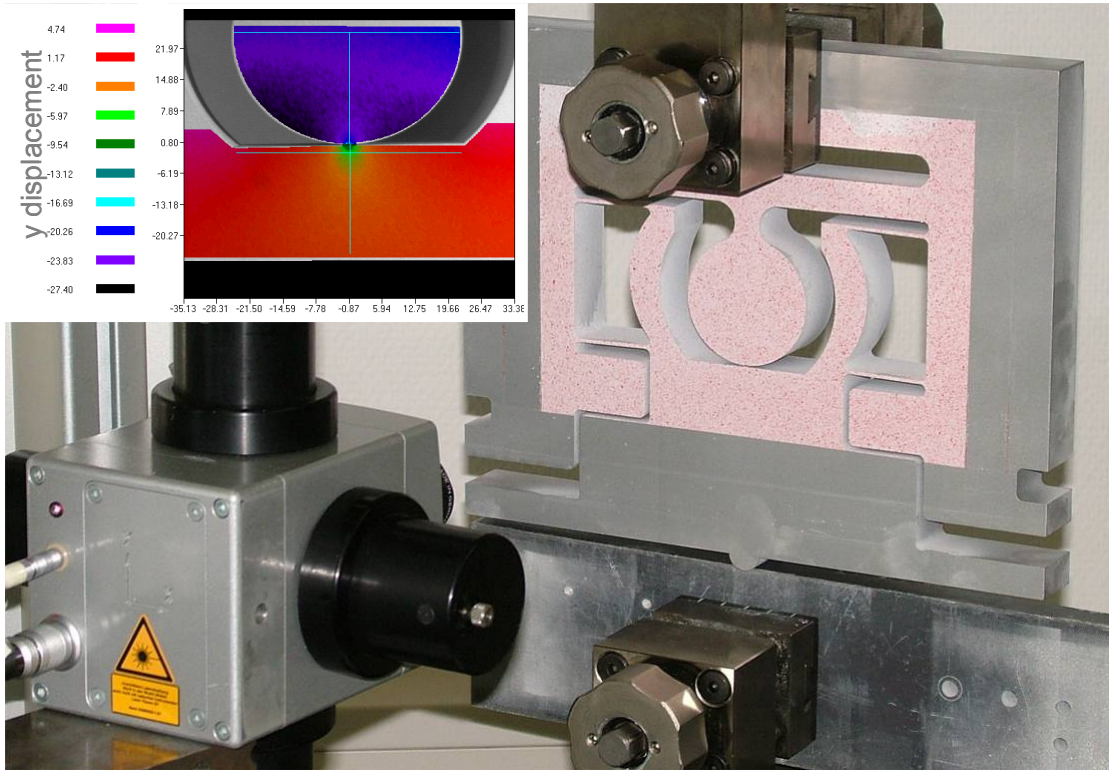


Figure 13 –A physical standardised test material (PSTM1) manufactured from aluminium with a disc diameter of 50mm and thickness of 25mm under test (upside down to reduce rigid body displacement in the gauge area) with an ESPI system (Dantec Dynamics GmbH Q300). Typical results are shown in the inset.

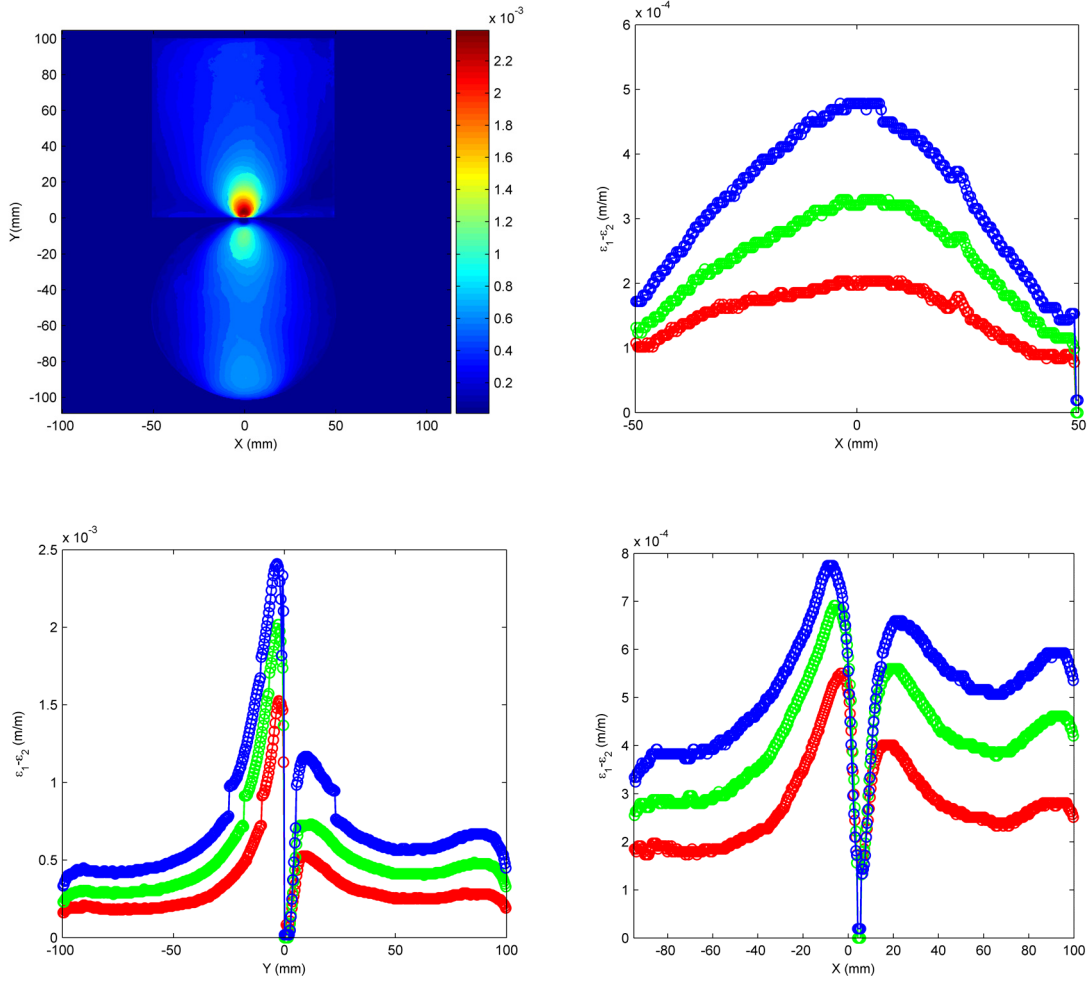


Figure 14 – A standardized test material with $D=100\text{mm}$ manufactured in epoxy resin using stereolithography being viewed in a reflection polariscope (*top left*) and the difference in principal strains along three lines through this data: $y = 0$ (*top right*), $x = 0$ (*bottom left*) and $y = (D/2 + 0.4a)$ (*bottom right*). In the plots data at compressive loads of 795N (red), 1590N (green) and 2395N (blue) is shown.